Annu. Rev. Biochem. 1990. 59:439 73

ANTIBODY-ANTIGEN COMPLEXES[1]

David R. Davies and Eduardo A. Padlan

Laboratory of Molecular Biology, National Institute of Diabetes, Digestive and Kidney Diseases, Bethesda, Maryland 20892

Steven Sheriff

Squibb Institute for Medical Research, Princeton, New Jersey 08543 4000

KEY WORDS: epitopes, complementarity, modeling, three dimensional structure, haptens

---

CONTENTS

INTRODUCTION

Antibodies are made in all vertebrates as part of the immune response to antigenic challenge by foreign substances. The diversity of this response is impressive: any foreign macromolecule can, under appropriate conditions, elicit an immune response. It has been estimated that humans can produce as many as 10 million different antibodies in the primary repertoire and that this may then be further expanded by several orders of magnitude through the effects of somatic mutation (1). In addition, the antibody response shows remarkable specificity, so that evidence of any significant amount of cross-reactivity between different antigens is usually taken to indicate close similarity of their structures. The manner in which diversity and specificity operate in the antibody molecule at the level of the three-dimensional structure, as determined by X-ray diffraction, is the subject of this review.

Antibodies were the first members of the immunoglobulin superfamily to be studied structurally. The domain structure observed in antibodies (2–7) has now been seen in many cell-surface proteins that function to control the movement and differentiation of many types of vertebrate cells (8, 9). Members of this family have characteristic domains of approximately 100 amino acids and often contain an internal disulfide loop of 40–70 residues. In those proteins where the three-dimensional structure is known, notably antibodies and the class I MHC antigens (10, 11), the tertiary fold of these domains has been very similar. The recently reported structure of the chaperone protein from *Escherichia coli*, PapD (154), is of particular interest since both domains of this structure have the immunoglobulin fold despite the absence of sequence similarity with the IgG CH2 domains.

Antibodies (see Figure 1) are multivalent molecules made up of light (L) chains of approximately 220 amino acids and of heavy (H) chains of 450–575 amino acids. The light chains contain two immunoglobulin domains; the N-terminal domain is variable, i.e. it varies from antibody to antibody, and the C-terminal domain is constant, i.e. it is the same in light chains of the same type. The heavy chains are made up of an N-terminal variable domain and three or four constant domains. The antibody fragment containing the associated variable domains of the light chain (VL) and of the heavy chain (VH) is called the Fv; the fragment containing the entire light chain and the VH and first constant domain of the heavy chain is called the Fab.

The combining site of antibodies is formed almost entirely by six polypeptide segments, three each from the light and heavy chain variable domains. These segments display variability in sequence as well as in number of residues, and it is this variability that provides the basis of the diversity in the binding characteristics of the different antibodies. These six hypervariable

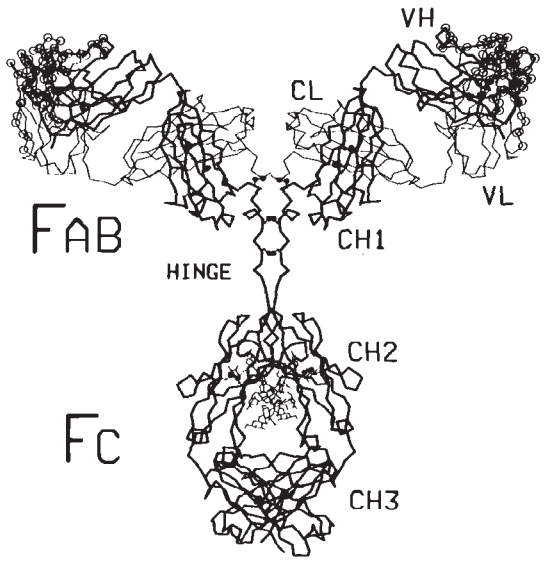

Figure 1 Line drawing of the alpha carbon trace of a model of human IgG1 (E. A. Padlan, unpublished). Thick lines show the heavy chain, thin lines the light chain. The various domains of the light and heavy chains are labeled (VL, VH, CH1, etc). The antigen binding fragment, Fab, and the Fc (consisting of the CH2 and CH3 domains of the two heavy chains) are labeled. The hinge is the heavy chain peptide segment joining the Fab and the Fc. It varies considerably in size in different antibody types. The hinge is often rich in proline and cysteine residues; the latter link the two heavy chains through symmetrical disulfide bonds. These interchain disulfide bonds, as well as those found in the domain interiors, are shown as filled circles. Carbohydrate has been found between the two CH2 domains in human IgG1 Fc (152), and is probably in a similar location in most of the other antibody classes. The two carbohydrate chains are drawn with thin lines.

The molecule was assembled from the Fab of KOL (153), a model of the octapeptide Pro Ala Pro Glu Leu-Leu-Gly-Gly, corresponding to residues 230–237 in the human IgG1 hinge (12), and the human IgG1 Fc of Deisenhofer (152).

segments are also referred to as the complementarity determining regions or CDRs (12).

The three-dimensional structure of antibodies has been the subject of numerous investigations (reviewed in 13–23), and crystal structures for intact immunoglobulins and for a variety of fragments are now available. More than a dozen Fab structures have been determined crystallographically and at least eight of those have been studied with bound ligand. Three Fab-ligand complexes involve small haptens [vitamin K_1OH (24), phosphocholine (25–27), and fluorescein (28)], and five complexes involve proteins [three with hen egg white lysozyme (29–31) and two with influenza virus neuraminidase (32–

34)]. The structures of Fabs with specificities for carbohydrates, DNA, and other molecules have also been determined, although at present only in the uncomplexed form.

The three-dimensional structures of antibodies and of antibody fragments have been reviewed extensively (13–23). Here, we concentrate on the interaction between antibody Fabs and specific ligands. We first consider the binding of antibodies to small molecules (haptens) and then to larger molecules (in particular, proteins). We then analyze the various antibody-ligand complexes of known three-dimensional structure looking at properties that define the specificity and strength of the interactions.

We also discuss briefly how the specificity of antibodies is being utilized for a variety of practical applications. For example, it has long been speculated that antibodies could be used as enzymes. Antibodies and enzymes share the ability for very specific binding. However, antibodies only bind to antigens, while enzymes bind substrates and catalyze their conversion to products. It was proposed 20 years ago by Jencks (35) that antibodies raised against transition-state analogues could have catalytic activity. This possibility has now been demonstrated, and antibody enzymes (abzymes) showing significant activity have been produced (36, 37).

Antibodies have many potential uses in diagnosis and in therapy and, with the advent of hybridoma technology (38), monoclonal antibodies of almost any desired specificity can be produced. However, the monoclonal antibodies that are more easily made are of rodent origin, and the long-term use of these antibodies in human subjects is blocked by the immune response of the host. Attempts have been made to circumvent these difficulties by the creation of chimaeric antibodies containing the constant domains of the host together with rodent variable domains (39–42). This 'humanization' of the more easily available rodent monoclonal antibodies has been further extended by the grafting of the rodent combining site structures to a human framework structure, making feasible the production of essentially human antibodies with designer binding properties (43–45).

For many of these applications a knowledge of the three-dimensional structures of particular combining sites is very helpful, but a crystallographic analysis of each antibody molecule is clearly impractical. The alternative is to use the existing structural information to model the new combining sites. The progress of these model building studies is discussed.

ANTIBODY BINDING TO SMALL MOLECULES

The first Fabs to be analyzed by X-ray diffraction were prepared from myeloma proteins. The antigenic determinants for these antibodies could only be inferred from binding studies using small molecules. Large numbers of

these immunoglobulins with known binding specificities were characterized and sequenced. The first two Fabs whose structures were determined, New, which was shown to bind to a vitamin K_1OH derivative (46), and McPC603, which binds to phosphocholine (47), were analyzed in both the complexed and uncomplexed forms (5, 7, 24–27, 48–50). Until the advent of hybridoma technology, these investigations provided the structural basis for understanding antigen recognition. They are still of considerable interest in showing how high binding and specificity can be produced for relatively small molecules.

In addition to New and McPC603, a third small-molecule-antibody complex, fluorescein bound to 4-4-20, has been recently determined in two laboratories (Ref. 28; M. Whitlow and K. Hardman, personal communication). As the complexes of New and of McPC603 have been reviewed previously (22), we describe them only briefly here.

McPC603 and Phosphocholine

McPC603 will precipitate with pneumococcus C polysaccharide (51), which contains phosphocholine. This precipitation is inhibited by phosphocholine (52), which binds to the McPC603 with a binding constant of 2.0×10^5 per mole (53). X-ray studies show that phosphocholine binds in a pocket in the McPC603 combining site with the choline buried and the phosphate on the surface (25–27). The phosphate group is within hydrogen bond distance of H-Arg52NH1 and H-Tyr330H. There is charge neutralization in that L-Asp91 is at the back of the pocket together with H-Glu35, which is one layer removed from contact with the positively charged choline. At the surface, H-Arg52 and H-Lys54 provide positive charges that complement the charge on the phosphate. The phosphocholine is in contact with only four of the six hypervariable loops: CDR1 of the light chain and all three CDRs of the heavy chain. There appears to be no conformational change upon binding phosphocholine, but this could be partially due to the presence of a sulfate ion from the crystallization medium, which is located in the phosphate-binding position (50).

New and Vitamin K_1OH

New was shown to bind to, among other ligands, the gamma-hydroxy derivative of vitamin K_1 with a binding constant of $1.7 \times 10^5\ M^{-1}$ (46). X-ray studies of the complex of Fab New with vitamin K_1OH revealed that the 2-methyl-1,4-naphthoquinone moiety of the vitamin K_1OH sits in a shallow groove between the heavy and light chains of approximately 16 Å × 7 Å and about 6 Å deep. The phytyl chain of the vitamin K_1OH runs along the surface of the antibody-combining site and contacts a number of residues. At the time of this investigation, the sequence of the New heavy chain had not been determined, so that the interaction between ligand and combining site could

not be described in detail. Amzel et al (24) estimate that the contact site consists of at least 10–12 residues and at least four hypervariable loops (L-CDR1, L-CDR3, H-CDR2, H-CDR3). The New–vitamin K_1OH coordinates are not available from the Protein Data Bank.

4-4-20 and Fluorescein

Anti-fluorescein antibodies have been found with affinities for fluorescein ranging from about 10^5 to 10^{10} M^{-1}. The 4-4-20 antibody binds fluorescein with an affinity at the high end of the range. Fluorescein consists of a xanthonyl moiety with enolic oxygens on each exterior ring and a phenyl carboxylate, which is attached through the ortho position to the central ring of the xanthonyl. The antibody is quite selective in that it does not bind the closely related rhodamine molecules, which have amino or diethylamino groups substituted for the enolic oxygens.

The fluorescein is bound with the planar xanthonyl ring at the bottom of a relatively deep slot formed by a network of tryptophan and tyrosine side chains. The phenylcarboxyl group is partially exposed to the solvent. The xanthonyl group is flanked by L-Tyr37 and H-Trp33. L-Trp101 makes up the floor of the combining site. The phenyl ring of the hapten is close to H-Tyr103; H-Tyr102 lines part of the boundary of the slot. The fluorescein is more than 90% buried by interaction with the 4-4-20 antibody and interacts with five of the hypervariable loops (L-CDR1, L-CDR3, H-CDR1, H-CDR2, H-CDR3) (28). The large xanthonyl moiety contributes more than 60% of the interactions with the antibody, which is consistent with that portion being 'immunodominant.'

One enolic oxygen on the xanthonyl moiety forms a hydrogen bond with L-His31NE2, and the other forms a salt link with L-Arg39NH2 and a hydrogen bond to L-Ser96OG. The negative charge on the carboxyl group that is part of the phenylcarboxylate is not neutralized, but faces towards solvent, and one of the oxygens hydrogen bonds to L-Tyr37OH. It is easy to understand why rhodamine analogues of fluorescein do not bind. First, the positive charge of the amino groups would create unfavorable interactions with L-Arg39. Second, in the case of diethylamino groups, there would be considerable steric problems in packing the ethyl moieties into the complex.

Animals are immunized to fluorescein by attaching it to a lysine group on keyhole limpet hemocyanin through an isothiocyanate group to the para position of the phenyl moiety. From this para position there is a channel in the complex through which the lysine from keyhole limpet hemocyanin could extend.

Other Fabs Binding to Small Ligands

A number of model antigens have provided experimental probes of antibody diversity, specificity, and genetic control of the immune response. One of the

most extensively studied model antigens has been the hapten, *p*-azobenzenearsonate. Recently the structure of Fab R19.9, which is specific for *p*-azobenzenearsonate, has been determined (54). This structure shows that nine aromatic residues, mostly tyrosines, in the antibody combining site are solvent exposed and could provide interactions with hapten.

Very recently two new hapten-antibody complexes have been determined. R. Fox, D. Leahy, and A. Brunger (personal communication) have determined the structure of AN02 Fab with the immunizing hapten 2,2,6,6-Tetramethyl-1-piperidinyloxy-dinitrophenyl bound. R. L. Stanfield, I. A. Wilson, and coworkers (personal communication) have determined the structure of an Fab both uncomplexed and complexed with a peptide that has the sequence of the C helix of myohemerythrin (55). Thus there will soon be an expanded view of hapten-antibody complexes, including the first examination of whether a peptide, which is helical in the native protein (56), maintains that structure when bound to antibody.

Wilson and coworkers have crystallized a number of other antibody-hapten complexes, which are suitable for structure determination. They have crystallized 17/9 Fab with and without the immunizing peptide, which is sequentially identical to residues 100–108 of subunit 1 of the influenza virus hemagglutinin. This sequence comes from the 'top' of the hemagglutinin, which is the immunodominant region (57). They have also crystallized the anti-progesterone DB3 Fab' both in the presence and absence of steroids, including progesterone, pregnanedione, and aetiocholanolane (58, 59). The space group and unit cell parameters are unaltered by the presence of the various steroids, although there is a change in crystal morphology.

ANTIBODY-ANTIGEN COMPLEXES

During the last three years there have been several structural investigations of monoclonal antibodies complexed with protein antigens. The structures analyzed include three complexes with lysozyme (D1.3, HyHEL-5, HyHEL-10) (Figure 2) and two complexes with the neuraminidase from influenza virus (32–34). In spite of their recent publication, these structures have already been extensively reviewed (33, 60 64), although there has been no comprehensive review of the results for all five complexes. In this section we first describe the individual results for each complex, and then discuss some of the common properties of the group.

The Anti-Lysozyme Complexes

These three structures form one subgroup among the complexes. The antigen, lysozyme, is a small 14.6-kd, rugged (65) glycosidase, with specificity for hexasaccharide having alternating beta-1,4-linked *N*-acetyl glucosamine and *N*-acetylmuramic acid residues (66). The crystal structure of tetragonal chick-

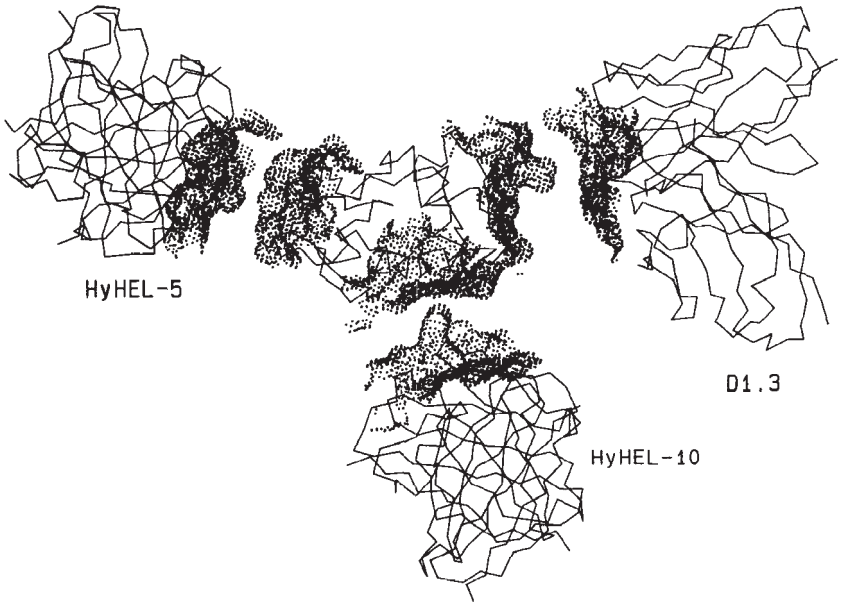

Figure 2 A composite of the Fvs of the three anti lysozyme antibodies: D1.3 (29), HyHEL 5 (30), HyHEL 10 (31) binding to lysozyme (75). For this picture the Fvs have been separated from lysozyme. C alpha representations are used for the Fvs and for lysozyme, and a dot representation is used for their interacting surfaces. It should be noted that the three epitopes are nearly non overlapping with only a small overlap between HyHEL 10 and D1.3.

en lysozyme was first determined in 1965 (67). Subsequently, the structures of several different crystal forms of chicken lysozyme have been determined (68, 69), as well as several closely related lysozymes from different sources (70, 71). The three-dimensional structure of lysozyme contains a mix of beta sheet and alpha helix. Across its middle it has an extensive cleft containing the catalytic residues, into which the hexasaccharide substrate binds. Lysozyme has been extensively used as a model antigen, both for antibodies and for T cell activation (72–75).

THE D1.3 COMPLEX The crystal structure of the antibody D1.3 complexed to lysozyme has been reported at 2.8 Å resolution (29). The interface between the antibody and antigen is extensive, involving 748 Å^2 of the solvent-accesible surface of the lysozyme and 680 Å^2 of the antibody (29). For the molecular surface the corresponding areas are 690 Å^2 and 680 Å^2, respectively (see Table 4, in a later section). The interface extends over maximum dimensions of 30 × 20 A. The fit between the two surfaces is very close with only one water molecule remaining in the interface.

Table 1 Antibody D1.3 residues in contact with lysozyme

	Antibody	Lysozyme
Light chain		
CDR1	His30	Leu129
	Tyr32	Leu25, Gln121, Ile124
FR2	Tyr49	Gly22
CDR2	Tyr50	Asp18, Asn19, Leu25
CDR3	Phe91	Gln121
	Trp92	Gln121, Ile124
	Ser93	Gln121
Heavy chain		
FR1	Thr30	Lys116, Gly117
CDR1	Gly31	Lys116, Gly117
	Tyr32	Lys116, Gly117
CDR2	Trp52	Gly117, Thr118, Asp119
	Gly53	Gly117
	Asp54	Gly117
CDR3	Arg99	Arg21, Gly22, Tyr23
	Asp100	Gly22, Tyr23, Ser24, Asn27
	Tyr101	Thr118, Asp119, Val120, Gln121
	Arg102	Asn19, Gly22

The epitope (Figure 3*a*) consists of two stretches of polypeptide chain, comprising residues 18 to 27 and 116 to 129, distant in sequence but adjacent on the protein surface (Table 1). The side chain of Gln121 projects outwards from the lysozyme and penetrates deeply into a pocket on the antibody, where the amide nitrogen makes a hydrogen bond with a main-chain carbonyl oxygen of L-Phe91. The pocket is lined by aromatic side chains of L-Tyr32, L-Trp92, and H-Tyr101. Replacement of Gln121 by His in several other avian lysozymes effectively abolishes the binding to the antibody.

All six CDRs of the antibody make contact with the lysozyme. In addition, there are two framework residues that are involved in contact, L-Tyr49 and H-Thr30. Of the 17 contacting residues, nine are aromatic, including five tyrosines.

No significant change in the conformation of the lysozyme is observed in the complex. In a recent report the structure of the unliganded D1.3 Fab is briefly described (76). This structure, currently under refinement, shows no significant change in the relative orientation of the VL and VH domains from the Fab complexed to the lysozyme, nor is there any change in the tertiary structure of the CDRs. There is a difference in the elbow bend (18) of the Fab, which is 172° in the complex vs 138° alone.

Also reported is the structure determination of a complex of the D1.3 Fab

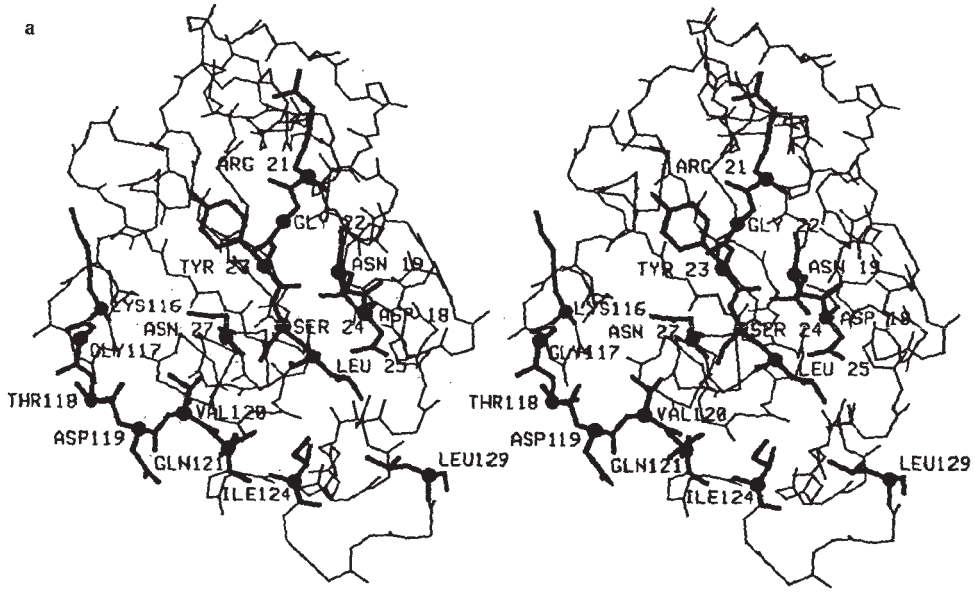

Figure 3a Stereo drawing of the lysozyme epitope for D1.3 defined in Table 1 (coordinates courtesy of Dr. R. Poljak). The contacting residues are labeled.

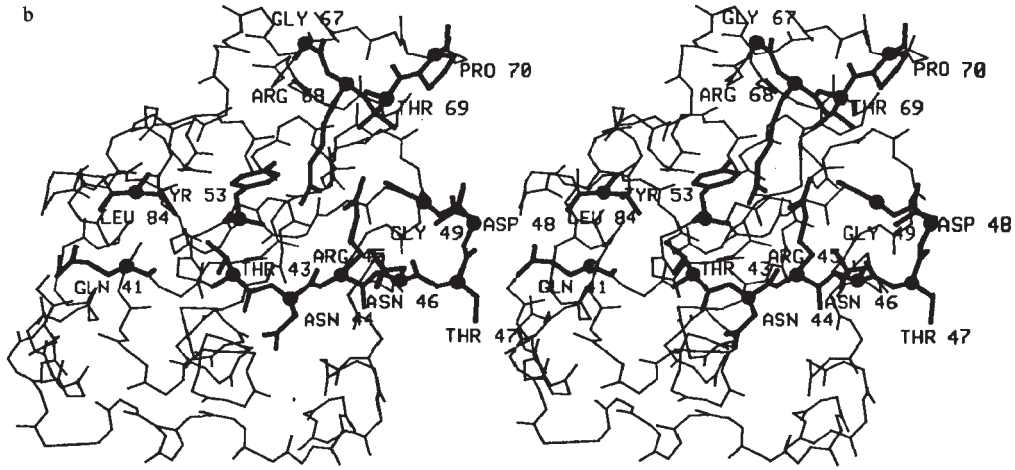

Figure 3b Stereo drawing of the lysozyme epitope for HyHEL-5 defined in Table 2. The contacting residues are labeled.

c

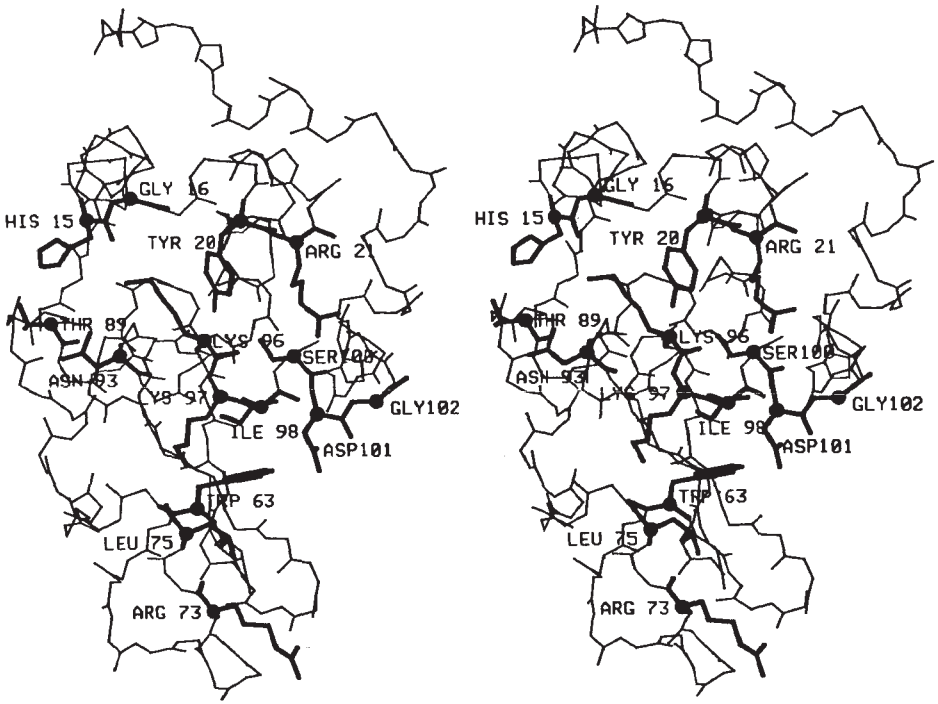

Figure 3c Stereo drawing of the lysozyme epitope for HyHEL-10 defined in Table 3. The contacting residues are labeled.

with its anti-idiotype, E225, Fab (76). Here too the structure is in the course of refinement, but the principal structural features can be described. Again there is no indication of significant conformational change in either the relative orientations of the VL and VH domains, or in the tertiary structure of the CDRs of D1.3. The elbow bend is 140° in this complex, almost indistinguishable from that of the uncomplexed D1.3. The idiotype recognized by E225 is largely centered on the VL domain, but with contributions from CDR3 and, to a lesser extent, CDR2 of VH.

THE HyHEL-5 COMPLEX The monoclonal antibody, HyHEL-5, complexed to lysozyme, has been determined in two different crystal forms (30). It binds to the opposite end of the lysozyme molecule from D1.3 (Figure 2). The epitope (Figure 3b) is made up of three segments of the polypeptide chain: residues 41–53, 67–70, and 84 (Table 2). In addition, several surrounding residues, while not in direct contact with the antibody, are partly buried by the interaction. This epitope includes Arg68, which, together with Arg45 forms a ridge on the surface of the molecule. Arg68 had been demonstrated by epitope mapping to be a 'critical' residue, replacement of which by a lysine led to a 1000-fold decrease in binding to HyHEL-5 (77).

Table 2 Antibody HyHEL 5 residues in contact with lysozyme

	Antibody	Lysozyme
Light chain		
CDR1	Asp31	Asp48
	Tyr32	Pro70
CDR2	Asp50	Pro70
CDR3	Trp91	Arg45, Gly49, Arg68
	Gly92	Arg45, Asn46, Thr47
	Arg93	Arg45, Asn46, Thr47
	Pro95	Arg45
Heavy chain		
CDR1	Trp33	Tyr53, Arg68
	Glu35	Arg68
FR2	Trp47	Arg45
CDR2	Glu50	Arg45, Arg68
	Ser55	Gln41, Leu84
	Ser57	Gln41, Thr43
	Thr58	Thr43
	Asn59	Thr43, Asn44
CDR3	Gly95	Arg68
	Tyr97	Gly67, Arg68, Thr69, Pro70

The antibody combining site contributes residues from all six of the CDRs to the contact with lysozyme (Table 2). There is also at least one framework residue, H-Trp47, that makes contact with lysozyme. In addition to many van der Waals' contacts, there are several salt bridges between the guanidinium groups of Arg45 and Arg68 and the carboxyl groups of H-Glu35 and H-Glu50. There are also 10 hydrogen bonds between uncharged groups of atoms. The contacting residues from the antibody include two tyrosines and three tryptophans.

The surface areas of the antibody and lysozyme in contact are about 750 $Å^2$ each. The interaction between the two surfaces shows good shape complementarity; there are only two water molecules remaining within the interface. The ridge on the lysozyme surface formed by the two arginine side chains fits into a groove on the antibody.

There does not appear to be any gross conformational change in the lysozyme as a result of binding; superposition of the bound and unbound lysozymes shows a root mean square displacement of the backbone atoms of 0.48 Å. The biggest C-alpha displacement is 1.7 Å for Pro70. The largest side-chain change occurs for Trp63 within the substrate binding groove where the indole ring system has rotated by about 180° about the CB-CG bond, even though it is not in contact with the Fab.

THE HyHEL-10 COMPLEX The monoclonal antibody HyHEL-10 binds to yet another part of the lysozyme surface (31) (Figure 2). The epitope is centered on the alpha helix running from residues 89 to 99, and can be regarded as containing this helix together with some surrounding residues. There are antibody contacts with Trp63 within the lysozyme groove and with residues on the other side of the groove from the helix. The area of lysozyme in contact with the antibody is 774 $Å^2$. In Table 3 the contacting residues between the antibody and the lysozyme are shown. In addition to 114 pairwise van der Waals' contacts, there are 14 hydrogen bonds. There is only one salt bridge, a weak hydrogen bond between the oppositely charged side chains of H-Asp32 and Lys97.

The surface of the HyHEL-10 that interacts with lysozyme is unusual in that it is not noticeably concave and contains no pronounced grooves or cavities. Instead it has a large protrusion consisting largely of the side chains of H-Tyr33, and H-Tyr53 that fit into the substrate-binding groove of lysozyme. The shape complementarity between the antibody and antigen is again remarkable, with no water molecules that can be detected within the interface.

The interacting surface of the antibody is rich in aromatic residues, particularly tyrosines, which make up 6 out of 19 contacting residues (Table 3, Figure 4). These tyrosines point outward from the combining site to make contact with the lysozyme.

Table 3 Antibody HyHEL 10 residues in contact with lysozyme

	Antibody	Lysozyme
Light chain		
CDR1	Gly30	Gly16
	Asn31	His15, Gly16, Lys96
	Asn32	Gly16, Tyr20
CDR2	Tyr50	Asn93, Lys96
	Gln53	Thr89, Asn93
CDR3	Ser91	Tyr20
	Asn92	Tyr20, Arg21
	Tyr96	Arg21
Heavy chain		
FR1	Thr30	Arg73
CDR1	Ser31	Arg73, Leu75
	Asp32	Lys97
	Tyr33	Trp63, Lys97, Ile98, Ser100, Asp101
CDR2	Tyr50	Arg21, Ser100
	Ser52	Asp101
	Tyr53	Trp63, Leu75, Asp101
	Ser54	Asp101
	Ser56	Asp101, Gly102
	Tyr58	Arg21, Ser100, Gly102
CDR3	Trp98	Arg21, Lys97, Ser100

No major conformational change takes place in the lysozyme upon binding. A comparison of the bound lysozyme coordinates with those of uncomplexed lysozyme shows a root mean square displacement of 0.47 Å for the alpha carbons, with significant deviations at residues 47, 101, and 102 of 1.44, 1.80, and 2.13 A, respectively. Larger deviations are found in the side chains, most notably that of Trp62 where the aromatic ring has been rotated by 150° about the CB-CG bond, presumably to avoid close contact with a tyrosine side chain of the antibody.

Although no structure is available for the uncomplexed antibody, Padlan et al (31) believe that no significant conformational change can have taken place because of the overall similarity of the HyHEL-10 domain structures to those of other Fabs and the similar ways in which the domains associate.

SUMMARY OF RESULTS FOR THE LYSOZYME COMPLEXES The three anti-lysozyme complexes described above have been reviewed (62). They have epitopes that are almost entirely non-overlapping; there is a small overlap between D1.3 and HyHEL-10 (Figures 2, 3), but Smith-Gill (private communication) has observed little or no functional competition. Together, these

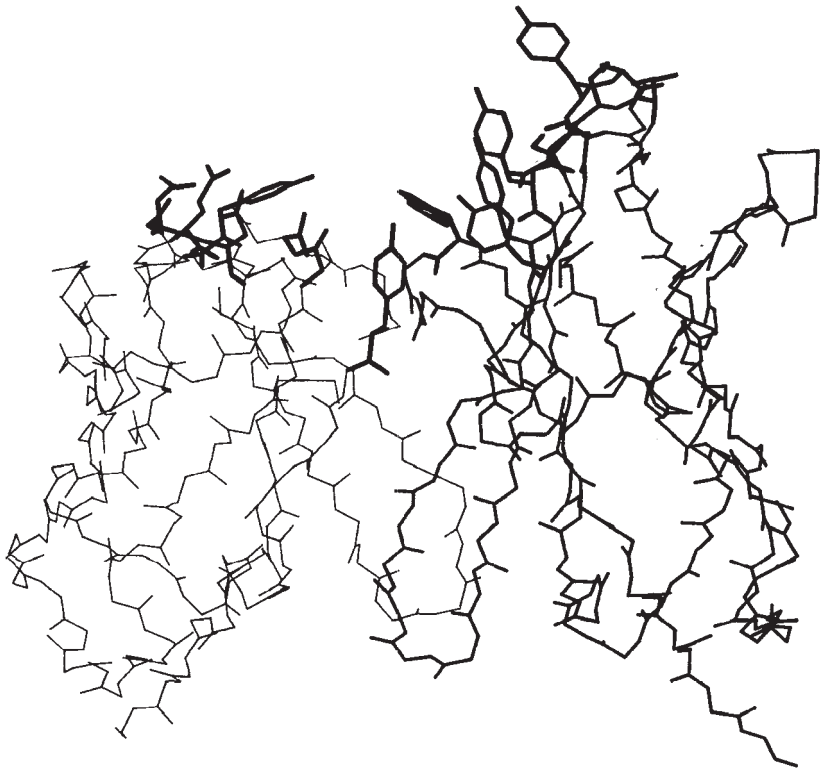

Figure 4 A line drawing of the HyHEL-10 Fv. The structure shown is that of the Fv in the complex, with the lysozyme removed. The combining site surface is at the top of the figure. Residues that contact the antigen are displayed with side chains; only the backbone is shown for the rest of the structure. VH is on the right, VL is on the left. Note the many aromatic side chains that protrude out to contact the antigen.

epitopes cover more than 40% of the lysozyme surface area. A comparison of the 'B' factor for lysozyme at different parts of the sequence with the positions of the epitope showed no particular correlation. This, together with the large total area covered by the three epitopes, was interpreted to mean that any part of the surface that is accessible to the antibody combining site is potentially antigenic, in agreement with Benjamin et al (74). The role of mobility in defining the antigenicity of regions of the protein surface has been extensively discussed recently by van Regenmortel (78) and by Getzoff et al (79, 80). The extent to which a correlation with mobility occurs has been deduced from experiments where the epitopes are defined largely by peptide mapping. It seems reasonable that when the antibody and antigen interact, some adjustment of the positions of the interacting residues, particularly the

side chains, will be observed, corresponding to induced fit. The regions most likely to show these changes will be those with the greatest mobility. However, any advantage gained in fitting these regions to the antibody will be at least partially offset by the entropic cost of immobilization upon forming the complex.

The conformational changes observed here for the backbone atoms of the lysozyme in the three anti-lysozyme complexes vary from very small for D1.3 (29), to a few angstroms for HyHEL-5 (30) and HyHEL-10 (31). The changes observed in the side chains are larger, and sometimes involve rotations of aromatic ring systems (HyHEL-5, HyHEl-10), supporting the contention that rearrangements of side chains sometimes occur in myohemerythrin (79, 80), with the effect of exposing otherwise buried groups to the antibody.

A striking feature of the interaction of these three antibodies with lysozyme is the shape complementarity of the two surfaces, as revealed by the almost total exclusion of water from the interface over an area of about 700 A^2 for both the antibody and antigen. This is a common feature of multisubunit protein interfaces as shown by X-ray analysis (81), and suggests that the water exclusion must play a significant role in stabilizing the complex (82).

The Antibody-Neuraminidase Complexes

The neuraminidase is one of two glycoproteins attached to the influenza viral membrane, the other being the hemagglutinin. It catalyzes the cleavage of terminal sialic acid from adjacent sugar residues. The neuraminidase and the hemagglutinin make up the antigenic surface of the virus, and changes in these proteins form the basis for evasion of immune recognition from previous infections.

The intact neuraminidase is a tetramer of molecular weight 240,000, which when solubilized with pronase, reduces to a 200,000-dalton head. The N2 enzyme subunit contains 469 amino acids and four carbohydrate molecules. The crystal structure of the N2 neuraminidase head has been determined (83). Each subunit of the tetramer is folded into an unusual array of six beta sheets, with each sheet having four antiparallel strands arranged consecutively. When viewed from the top surface of the molecule the sheets have the appearance of the six blades of a propeller. The active site contains a large sialic acid–binding pocket in the middle of each subunit surface.

THE NC41 COMPLEX The structure of the neuraminidase complexed to a monoclonal antibody Fab, NC41, has been reported (32), and refined to 2.9 Å resolution (33). The epitope on the neuraminidase involves five segments, which contribute 22 residues in direct contact and five that are partly buried. There are also partially buried atoms in five residues from two other segments and in two sugar residues from the carbohydrate of a neighboring subunit.

The antibody combining site contributes 20 contacting and 12 partly buried residues. The CDR1 of the light chain does not make contact with the neuraminidase, and as a result the heavy chain has more interactions than the light chain. CDR3 of the heavy chain has the most buried surface area, making up approximately 30% of the total. Three framework residues are in contact, L-Tyr49, H-Thr28, and H-Thr30.

The buried surface area is significantly greater than for the lysozyme complexes, being about 878 A^2 for the neuraminidase and 885 $Å^2$ for the Fab. There is a good fit between the two surfaces, with no water molecules buried within the interface.

Possible changes in the antibody upon forming the complex were suggested by Colman et al (32) in the absence of the uncomplexed antibody structure. Small differences in the position of VH relative to VL in the different Fab structures had been previously noted and were attributed to the effect of interacting hypervariable residues (reviewed in 22). Colman et al (32, 63) proposed that the binding of antigen could also produce a displacement of the variable domains from each other. At that time the position of VH relative to VL for NC41 in the complex appeared to be an outlier in the group of Fab structures, and it was proposed that this difference in structure might have occurred as a result of antigen binding. However, the recently reported structure of an uncomplexed Fab, R19.9 (54), has an even bigger difference in the relative orientation of VL and VH than does NC41. This emphasizes the need for direct experimental observation from an analysis of the uncomplexed Fab structure. This is an important issue to resolve because seemingly small changes in the orientation of VH relative to VL can produce quite big modifications of the combining site, thus significantly enlarging the repertoire of specificities, although presumably at a cost of reduced binding energy.

THE NC10 COMPLEX A preliminary structure has been reported for a second monoclonal antibody Fab, NC10, complexed with the neuraminidase N9 isolated from whales, that differs by 14 amino acids from the tern neuraminidase used in the NC41 complex (34). The epitope approximates that of the NC41 complex, but the antibody Fv is rotated through about 90° from the position adopted by the NC41 Fv. Also, the relationship of the antibody to the neuraminidase surface is different: in NC41, L-CDR1 is the most remote from the epitope, while in NC10, L-CDR2 and H-CDR1 are the most distant. This structure is still in the course of refinement (33).

Comparison of the Neuraminidase and Lysozyme Complexes

The NC41-neuraminidase complex forms a more extensive interface than that between D1.3, HyHEL-5, and HyHEL-10 and lysozyme. Tulip et al (33) note that although the surface area is somewhat increased, as well as the number of

van der Waals' contacts, the number of hydrogen bonds and salt bridges is about the same. However, using different criteria, W.Tulip and S. Sheriff find rather more hydrogen bonds in the NC41 complex than in the lysozyme complexes (Table 4).

In the NC41 complex the antigen does not make contact with the CDR1 of the light chain. This CDR is described as 'hanging over' the active site in a position where it could possibly interfere with the access of substrate to the enzyme.

In all the complexes there is remarkable shape complementarity between the antibody and antigen surfaces, with exclusion of all or almost all water molecules from the interface.

Antibodies with Specificities for Other Large Molecules

The structures of several other Fabs that bind to large molecules have been determined: J539, CF4C4, HED10, BV04-01, Jel 42, Jel 72, and Jel 318.

J539 and CF4C4 have specificities for carbohydrate. The structure of J539, which is specific for beta(1-6)-D-galactan, has been determined at 2.6 Å resolution (84) and further refined with additional data (T. N. Bhat, E. A. Padlan, D. R. Davies, unpublished results). The antibody combining site is in close proximity to the constant regions of another molecule, and this presumably inhibits galactan binding in the crystal.

The antibody CF4C4 is specific for Lewis *a* human blood group determinant Gal beta 1→3[Fuc alpha 1→4]GlcNAc. The structure of the Fab of CF4C4 has been determined to 3.0 Å resolution by molecular replacement, although at this time only a C alpha trace is known (85).

HED10 and BV04-01 are both auto-immune antibodies that bind to single-stranded poly(dT). The specificity of HED10 is apparently for four consecutive bases, but recognition of two phosphates is thought to be important because the binding constant is dependent on ionic strength. The antibody was derived from mice, which develop a disease resembling human systemic lupus erythematosus. In humans, systemic lupus erythematosus often results in a higher serum titer of anti-DNA antibodies. The structure of HED10 has been determined by molecular replacement at 3.0 Å resolution (86). Further structural work on this protein was inhibited by a lack of a complete sequence for VL and VH, but most of the sequence has become available and the structure has been refined (W. Anderson, personal communication).

BV04-01 antibody also recognizes single-stranded poly(dT), but here phosphate groups are less important in the interaction (87). BV04-01 Fab crystallizes nearly isomorphously with the anti-fluorescein 4-4-20 Fab and has a very similar structure except for CDR3 of the heavy chain, which is three residues longer (28).

Anderson and coworkers have crystallized two anti-DNA Fabs, Jel 72 and

Table 4 Antigen-antibody complexes: buried surface and contacts[a]

Antigen				Antigen in complex						Antibody	
				buried				in contact			
Name	M_r	Surface area, Å^2	atoms	Surface area, Å^2	%	atoms	residues	atoms	residues	Name	Ref.
phosphocholine	169	169	11	137	81	10		9		McPC603	(27)
fluorescein	320	282	25	266	94	24		21		4-4-20	(28)
lysozyme	14,000	5,436	1,000	750	14	86	24	46	14	HyHEL-5	(30)
		5,414	1,001	774	14	98	27	49	15	HyHEL 10	(31)
		5,564	1,000	680	12	89	27	43	15	D1.3	(29)
neuraminidase	50,000	14,648	3,164	879	6	113	32	63	21	NC41	(33)

Antigen	Antibody in complex							Complex			
	buried				in contact						
	Name	Surface area, Å^2	atoms	residues	atoms	residues	CDRs	VDW contacts	H bonds	salt links	K_a M^{-1}
phosphocholine	McPC603	161	27	12	22	8	4	30	2	3	1.7×10^5
fluorescein	4 4-20	308	49	15	36	11	5	65	5	1	3.4×10^{10}
lysozyme	HyHEL 5	746	91	28	45	17	6	74	10	3	2×10^{10}
	HyHEL 10	721	99	30	59	19	6	111	14	1	5×10^9
	D1.3	690	90	22	43	14	6	75	15	0	1×10^9
neuraminidase	NC41	886	112	32	65	21	5	108	23	1	

[a] All surface areas were calculated using Program MS (149), with a 1.7 Å probe sphere and van der Waals radii from (148). Contacting residues are defined as in (56). These numbers may be at variance with those found by the original authors owing to different definitions of contacting residues. Values for the neuraminidase under Antigen are given for a monomer. All values for the neuraminidase were kindly provided by William Tulip (personal communication). The K_a has not been determined for neuraminidase binding to NC41.

Values for D1.3 were calculated from coordinates given to us by Roberto Poljak. Values for 4-4-20 were calculated from coordinates given to us by Allen Edmundson and James Herron (these coordinates have been deposited in the Protein Data Bank, but had not yet been processed by the Data Bank). Differences in the number of atoms for lysozyme reflect whether a carboxy terminal oxygen was included in the model. Differences in the surface area for lysozyme are due to differences in conformation of surface residues.

Jel 318 (88). Jel 72 is specific for right-handed duplex poly(dG)- poly(dC), and Jel 318 binds triple-stranded DNA poly[d(Tm^{5}C)]-poly[d(GA)]-poly[d(m^{5}C$^+$T)]. They have recently determined the structures of both Jel 72 and Jel 318 by molecular replacement (W. Anderson, A. Muir, personal communication).

Delbaere and coworkers (89) have determined the structure of Jel 42 Fab, which is specific for the histidine-containing protein (HPr), which is a small protein involved in the phosphoenolpyruvate:sugar phosphotransferase system of *E. coli*. Very recently, they have obtained crystals of the complex between HPr and Jel 42 Fab (90). It is therefore likely that an antibody-antigen complex with a different protein antigen will be available soon.

STRUCTURAL ASPECTS OF ANTIBODY-ANTIGEN COMPLEXES

In general, two macromolecules in solution have to overcome large entropic barriers before they can form a tight association. There is the loss of the entropy of free rotation and translation of the separate molecules, and there is the loss of conformational entropy of mobile segments and of side chains upon binding. On the other hand, entropy is gained when water molecules are displaced from the surfaces that become the new interface. This latter effect is quite significant and, in the structures observed by X-ray analysis, it appears that water molecules are almost totally excluded from the interface by the close shape complementarity of the surfaces.

Enthalpic contributions arise from van der Waals interactions together with the more specific hydrogen bonds and salt bridges. All of these interactions have been observed in the complexes described above. The van der Waals' and the ionic interactions in the various antibody-ligand complexes are summarized in Table 4. In the four antibody-protein complexes analyzed, there are from 75 to 110 atom pairs in contact. Further, there are between 10 and 23 hydrogen bonds and as many as three salt bridges. Although the hydrogen bonds between antibody and ligand replace hydrogen bonds to water molecules, so that the net enthalpy change is less than if they were being made in vacuum, taken together they make a significant contribution to the enthalpy.

Table 4 also compares the degree of surface interaction between antibodies and ligands in the complexes for which three-dimensional coordinates are available. As one would expect, the larger the ligand the more surface area is involved on both molecules, although the surface area does not increase proportionately to the total surface area of the ligand. The neuraminidase-NC41 complex buries approximately 20% more surface on both antibody and antigen than each of the three lysozyme antibody complexes, despite the

neuraminidase having more than 2 ½ times the surface area of lysozyme. This suggests that for protein antigens, the size of the antibody combining site becomes the determining factor in antibody-antigen interactions.

The two small molecule ligands bind in a pocket (phosphocholine in complex with McPC603) or in a slot (fluorescein in complex with 4-4-20), whereas the protein antigen complexes with antibodies have broad and relatively flat surfaces of interaction. The two small ligands are almost entirely buried in the interaction with antibody, and this is reflected in the large percentage of atoms that are at least partially buried or are, using a more restrictive definition of interaction (56), in contact with the antibody. On the other hand in the protein antigens, we find about 25 residues and about 90 atoms at least partially buried in the lysozyme epitopes and a rather smaller number of residues (~15) and atoms (~46) actually in contact with the antibody. The corresponding numbers in the case of neuraminidase, which are somewhat larger, reflect the larger surface of interaction. On the antibody side, we see nearly the same number of atoms and residues involved as were involved on the antigen. It is interesting that although the surface of interaction between the neuraminidase and the NC41 Fab is somewhat larger than for the lysozyme Fab complexes, only five of the six hypervariable loops or CDRs are involved in the former.

We can examine the types of contacts the various antigens make with their respective antibodies and compare those with the K_a of the complex. It can be seen that hydrogen bonds and salt links (interactions between charged moieties) are important, but not in a linear way. For example, the binding of fluorescein to 4-4-20 has the highest affinity constant [although there are reasons to believe that the affinity constant for HyHEL-5 and lysozyme may be underestimated (S. J. Smith-Gill, personal communication)], despite the fact that only one salt link and five hydrogen bonds are observed in the complex. However, there are nearly as many van der Waals' contacts as for two of the lysozyme Fab complexes, and these contacts must play an important role. On the other hand, phosphocholine makes several salt links and two hydrogen bonds and binds with a rather low affinity. Obviously a crude accounting of contacts is not sufficient. Novotny et al (91) have attempted to estimate binding energies in several of the cases (McPC603, D1.3, HyHEL-5) and find that they are able to determine the most important residues in an energetic sense, but have somewhat more limited success in predicting affinity constants, especially in the case where paired charges are buried in an apolar environment.

The contributions of the VH and VL and of the different CDRs can be analyzed separately. When we examine the influence of the light and heavy chains on binding to antigen we see a rather consistent result. In the four antibodies (HyHEL-5, HyHEL-10, D1.3, and NC41) to protein antigens, the

Table 5 Contributions of light and heavy chains to buried surface and contacts[a]

	buried				in contact				
	surface A^2	% total	atoms	residues	atoms	residues	VDW contacts	H-bonds	salt links
McPC603									
Light	76	47	12	6	8	4	11	0	0
Heavy	85	53	15	6	14	4	19	2	3
4-4-20									
Light	122	40	17	7	12	5	19	4	1
Heavy	186	60	32	8	24	6	46	1	0
HyHEL 5									
Light	307	41	29	12	20	7	33	4	0
Heavy	440	59	52	16	25	10	41	5	3
HyHEL 10									
Light	310	43	44	14	21	8	42	7	0
Heavy	411	57	55	16	39	11	69	7	1
D1.3									
Light	295	43	38	10	20	6	34	3	0
Heavy	385	57	52	12	23	8	41	12	0
NC41									
Light	386	44	51	13	29	11	42	11	0
Heavy	500	56	62	19	36	10	66	12	1

[a]Values were calculated as in Table 4.

Values for 4-4-20 were calculated from coordinates given to us by Allen Edmundson and James Herron (these coordinates have been desposited in the Protein Data Bank, but had not yet been processed by the Data Bank). Values for D1.3 were calculated from coordinates kindly provided to us by Roberto Poljak. Values for the neuraminidase were kindly provided by William Tulip (personal communication) and refer to the structure reported in (Tulip, Ref. 33)

light chain contributes from 41 to 44% of the surface area, and the heavy chain contributes from 56 to 59% of surface area (Table 5). 4-4-20 binding to fluorescein and McPC603 binding to phosphocholine fall only slightly outside the range. If one looks at the number of atoms and residues either at least partially buried or in contact with the antigen one sees much the same story. However, the number of hydrogen bonds and salt links does not always show the same bias. For example, 4-4-20 has four hydrogen bonds and one salt link from the light chain and only one from the heavy chain. HyHEL-10 and NC41 are relatively evenly divided between the two chains in terms of hydrogen bonds and salt links. On the other hand McPC603 and D1.3 favor the heavy chain in terms of hydrogen bonds and salt links much more than surface area would suggest.

If one looks at the importance of individual hypervariable loops, one finds that any hypervariable loop can be important. For example, L-CDR2 is not even buried in the complexes of McPC603 and 4-4-20, is the least important

CDR in HyHEL-5 and D1.3, and is of middling importance in HyHEL-10. However, in NC41, it is second only to H-CDR3 and if one includes the sequentially contiguous residues in L-FR2 then it is nearly of equal importance. There is some preference for either L-CDR3 or H-CDR3 to play a large role, for example, in D1.3, where H-CDR3 includes more than one quarter of the bound surface and 9 of 15 hydrogen bonds in the complex. On the other hand, in HyHEL-10, H-CDR3 is the least important hypervariable loop by any of the criteria examined.

The specificity of the antibody-antigen interaction might be regarded as a paradigm for molecular recognition in general. The specificities of these interactions are believed to result from the complementarity of the interacting surfaces. The investigations reviewed here confirm that there is remarkable shape complementarity; depressions on one surface are filled by protuberances from the other, leaving no holes large enough for even water molecules. Hydrogen bonding is another factor that makes the interaction specific. Of particular relevance here is the directionality of the hydrogen bonds, necessitating a hydrogen bond receptor within a certain distance and within a certain solid angle of the hydrogen bond donor in order to form a strong bond.

The interactions of oligomeric proteins have been examined by Janin et al (151). They find that dimer formation can involve an extensive area of interaction, ranging from 700 $Å^2$ to more than 4000 $Å^2$. The antibody-antigen surface area occupies the lower end of this range. They also find that the interacting surfaces tend to be quite hydrophobic, with an average of one hydrogen bond per 200 $Å^2$. In this respect, the antibody-antigen interfaces differ, with an average of about a dozen hydrogen bonds. This difference occurs presumably because the protein surface that is combining with the antibody is one that is normally exposed to solvent and therefore contains a significant content of polar residues.

The antibody combining site also differs from a typical oligomeric protein interface. In D1.3 and HyHEL-10 there are large numbers of aromatic residues present on the surface, particularly tyrosines (29, 31). An abundance of aromatics had also been observed in McPC603 (50), and more recently in R19.9 (54). Padlan (92) has analyzed the properties of these residues and demonstrated that they have another unusual feature, namely solvent exposure. The tyrosine and tryptophan side chains in the antibody combining sites are more exposed to solvent than those in the framework part of the variable domains, and also than those in other proteins. The exposure of these aromatic residues makes them available for ligand interaction. They can contribute significantly to the free energy of binding because of their large surface areas, and because they have relatively low conformational entropy, resulting in a lower entropy change when they become immobilized in the interface.

ANTIBODY ENGINEERING

Considerable attention has recently been directed towards the design of engineered antibodies for use in diagnosis and therapy (39–45, 93–96). This includes the synthesis of single-chain Fvs, sometimes attached to other molecules, with the intention of using the recognition part of the antibody molecule to provide specificity without having to include the constant domains. The uses of such Fvs are many. They can help to reduce the high background present in the imaging of tumors, which is partly due to the binding of the heavy chain constant region to nontumor cells (cf. 94). They can also be used as a vehicle for introducing toxins into cells having specific cell surface antigens (93). Also, for those uses that simply require strong binding to specific targets, where the effector functions that require the rest of the antibody molecule are not needed, single-chain Fvs have been demonstrated to be almost as effective as intact antibodies and will be less immunogenic.

Various linkers have been used to join the two variable domains. Bird et al (94) constructed genes for VL joined to VH by different linkers ranging from the 18 amino acids, KESGSVSSEQLAQFRSLD, to 14 amino acids in EGKSSGSGSESKST. Huston et al (95) and Chaudhary et al (93) used a 15 amino acid linker to join VH to VL with the sequence $(GGGGS)_3$. The affinities measured were fourfold lower for the linked Fv compared with the Fab fragment of an anti-bovine growth hormone (94), sixfold lower for an anti-digoxin vs the Fab (95), and threefold lower for anti-Tac(Fv) conjugated to two domains of *Pseudomonas* toxin (93).

Considerable progress is also being made in constructing chimaeric antibodies for potential use in therapy. Because it is difficult to make human monoclonal antibodies, and because antibodies from other species produce an immune response in the human host and therefore have limited therapeutic value, recombinant DNA technology has been used to produce antibodies with Fvs from the mouse coupled to human constant domains (40, 42, 96). Winter and coworkers have demonstrated the feasibility of grafting mouse CDRs onto a human heavy chain framework. When these chains were combined with the autologous mouse light chains the ligand-binding characteristics were retained (43, 44). Antibodies were also constructed in which the six hypervariable regions of a rat antibody directed against human lymphocytes were introduced into the framework residues of human variable domains (45), thus creating a modified human antibody with the binding specificity of the rat antibody.

CATALYTIC ANTIBODIES

The notion of complementarity between antibody and antigen (97) and the suggestion that the enzyme active site serves as a template for the transition

state (98) led to the proposal that antibodies directed against transition-state analogues could have enzymatic activity (35).

The esterase-like activity of specific polyclonal and monoclonal antibodies to dinitrophenyl (99, 100) and to steroid (101, 102) esters was noted early on. The antibody-induced hydrolysis, however, was found to be stoichiometric rather than catalytic.

Catalysis by antibodies was first demonstrated by Tramontano et al (103), who used phosphonate esters as haptens to elicit antibodies capable of hydrolyzing carboxylic esters, and by Pollack et al (104), who used the myeloma protein MOPC167, which binds the transition-state analogue *p*-nitrophenylphosphorylcholine with high affinity, to catalyze the hydrolysis of the corresponding carbonate. One of the antibodies generated by Tramontano et al (103) accelerated ester hydrolysis by a factor of 960; Pollack et al (104) found that MOPC167 accelerated the hydrolysis of nitrophenyl carbonates by a factor of at least 770.

Since then monoclonal antibodies have been elicited that catalyze a variety of chemical reactions, including aryl and alkyl ester hydrolysis (105, 106), carbonate hydrolysis (107), a stereospecific cyclization (108), a stereospecific Claisen rearrangement (109–111), amide bond hydrolysis (112), bimolecular amide formation (113, 114), photocleavage of thymine dimers (115), redox reactions (116), peptide cleavage (117), and a beta-elimination reaction (118). In one case, an antibody raised to a phosphonate ester accelerated the hydrolysis of carboxyl esters by 6.25×10^6 (105), which is in the range of those for known esterolytic enzymes. A recent study has reported the isolation of a human autoantibody that has catalytic activity against a vasoactive intestinal peptide (119).

Deliberate attempts have been made to introduce specific groups into the antibody combining site for greater or more specific catalytic activity. For example, introduction of a thiol group in the combining site of the dinitrophenyl-binding myeloma protein MOPC315 resulted in an antibody that accelerates ester cleavage 60,000-fold (120). Metal cofactors have been successfully introduced in antibody combining sites by the judicious design of the immunizing hapten (117). Similarly, a catalytic carboxylate residue was successfully generated in an antibody combining site by exploiting the anticipated charge complementarity between immunizing hapten and elicited antibody (118).

Since antibodies can be elicited against practically any structure, the possibility exists for the design and production of catalysts, i.e. catalytic antibodies, with virtually unlimited specificities. Such antibodies could have many industrial and medical applications (36, 37, 121, 122).

MODELING OF ANTIBODY COMBINING SITES

The high degree of similarity among the immunoglobulin domains in sequence and in three-dimensional structure has been an incentive for the modeling of immunoglobulin variable and constant fragments and of other molecules of the immunoglobulin supergene family. In particular, many models have been built of antibody combining site structures. In some cases, crystallographic analyses have permitted the comparison of the modelled structures with X-ray results.

The first modeling attempt was made by Kabat & Wu (123), who proposed the backbone structure of a variable domain on the basis of its amino acid sequence; their modeling procedure used phi, psi angles from corresponding tripeptides in proteins of known structure. The model that they proposed did not agree with the later X-ray results.

All subsequent attempts at model building were made after three-dimensional structures of immunoglobulins had become available. By then, it had become apparent that the tertiary structures of the homologous domains, especially the nonhypervariable or framework regions, were very similar and that the mode of association of the paired domains was essentially invariant. Accordingly, all modeling attempts since then have assumed the same framework structures for VL and VH, as well as the same quaternary association of these domains as found in the crystal structures. With regard to the modeling of the CDRs, two approaches have been taken. One approach uses a known CDR structure as a template; the other attempts to predict the CDR structure de novo on the basis of energetic considerations.

Template-Based Predictions

After they had determined the structure of Fab NEW, Poljak et al (48) tried to visualize the effect of replacing the combining site residues of NEW with the corresponding amino acids from the DNP-binding MOPC315. The combining site that could result was found to have many aromatic residues that could interact with the DNP moiety.

The first structure-based modeling of an antibody combining site was done by Padlan et al (124), who constructed a physical model of the Fv of MOPC315. The results of several crystallographic analyses that had been done by then (4–7, 48, 125) and the quantitative comparison of these results (20, 126) formed the basis of the modeling procedure. In constructing the model of MOPC315 Fv, Padlan et al (124) assumed that (*a*) the framework structures of the VL and the VH domains of MOPC315 were essentially the same as those of the domains of the mouse phosphocholine-binding im-

munoglobulin McPC603, (*b*) the quaternary association of the VL and VH domains of MOPC315 was the same as that found in McPC603, and (*c*) the CDRs of MOPC315 would have the same backbone conformations as those CDRs from other structures that had the same number of amino acid residues. Sequence similarity, where it occurred, was taken into account in building loop structures for which no suitable starting model was available. Insertions and deletions were made in such a manner as to maximize structural stability, and phi and psi peptide angles were maintained within reasonable limits. The interaction between loops was maximized, leaving no large holes in the domain interior, while minimizing steric hindrance between groups (124). The modeling, which included an attempt to position DNP in the combining site, was able to explain, at least qualitatively, most of the data on the interaction of DNP with MOPC315. This model of the combining site of MOPC315 was later refined on the basis of NMR data (127, 128).

The same basic procedure was used in the modeling of the combining site structures of the rabbit BS-5 anti-polysaccharide antibody (129), the inulin-binding EPC109 mouse myeloma protein (130), and the W3129 and 19.1.2 mouse anti-dextran antibodies (131). Very similar assumptions were used by Feldmann et al (132) in their modeling of the Fv of the galactan-binding mouse immunoglobulin J539 [later energy-minimized by Mainhart et al (133)], by Smith-Gill et al (134) in their modeling of the Fv of the lysozyme-specific HyHEL-10 antibody, and by de la Paz et al (135), who built models of three antibodies specific for an antigenic disulfide loop of lysozyme. In addition to length, de la Paz et al (135) used sequence similarity in choosing the CDR structures for use as templates in their modeling.

Chothia et al (136) built three models of the Fv of the anti-lysozyme D1.3 antibody. One model was built on the basis of the results of a detailed structural analysis and comparison of the hypervariable loops of antibodies of known three-dimensional structure. The other two were built using conformational energy calculations based on known X-ray structures. One of the latter models was based exclusively on the structure of McPC603, which is the molecule of known structure having the highest sequence similarity with D1.3 in both variable domains; the necessary insertions and deletions were made on the McPC603 template, and the resulting structure was subjected to energy minimization. The other model was built by merging features from three known Fab structures, selecting regions that bore the highest sequence similarity with D1.3, followed by energy minimization. The hypervariable loop designations used by Chothia et al were based on conformational differences observed in the crystal structures of various Fabs; these designations differ from those based on sequence variation (12).

De Novo Modeling

The first attempt to predict CDR structures de novo was made by Stanford & Wu (137), who constructed a model of the backbone structure of the combining site of MOPC315 on the basis of amino acid sequence and steric considerations. These authors assumed the same framework structure for MOPC315 as that found in Fab NEW (49) and used the predictive method of Kabat & Wu (123) to construct models of the CDRs. Phi and psi angles for tripeptides were obtained from known protein structures, relying mostly on beta-sheet proteins, and these angles were imposed on the segment being constructed based on its sequence. The peptide angles were allowed to vary from the initial values by as much as 30° in 5° intervals. The large number of resulting possible structures was reduced by imposing the conditions that the ends of the modelled CDRs should fit onto the assumed framework structure and that nonbonded atoms should not come within allowed minimum contact distances based on normally accepted van der Waals' radii. The CDRs near the center of the combining site were constructed first, those on the periphery last, i.e., L-CDR3, H-CDR3, H-CDR1, L-CDR1, H-CDR2, and L-CDR2, in that order. The success of their predictions could not be assessed since the three-dimensional structure of MOPC315 Fv is not yet available.

A related procedure was used by Bruccoleri et al (138) to reconstruct the crystallographically determined hypervariable loops of McPC603 and HyHEL-5. These authors generated all the possible conformations for each loop by imposing peptide dihedral angles that are energetically accessible to each residue in the sequence, sampling torsional space at 30° intervals. Here also, the number of possible structures was limited by imposing the conditions that the ends of the loops should fit onto the framework and that bad steric contacts are avoided. Both *cis* and *trans* peptide configurations for proline were considered. The innermost hypervariable loops were constructed first, the outermost last, so that the order of reconstruction was L-CDR2, H-CDR1, L-CDR3, H-CDR2, H-CDR3, then L-CDR1; these hypervariable loop designations differ from those based on sequence variation (12) and from those chosen by Chothia et al (136) on the basis of structural variation. The rms deviation from the X-ray structure of the backbones of the reconstructed hypervariable loops of McPC603 ranged from 0.7 Å to 3.8 Å; those for HyHEL-5 ranged from 0.4 Å to 2.1 Å.

A somewhat different approach was taken by Fine et al (139), who modelled four of the CDRs of McPC603, namely: H-CDR1, H-CDR3, L-CDR2, and L-CDR3. These authors generated a large number of random conformations for the backbone of each of the four CDRs, subjecting these conformations to molecular dynamics and/or energy minimization and then

selecting the lowest energy conformations for further characterization of side chain conformations. The random structures were generated such that they all fit onto the framework with correct geometry. In generating the loop conformations, random values were first assigned to each phi and psi peptide angle along the backbone, then these angles were adjusted as minimally as possible in an iterative procedure to produce the desired fixed-end conditions. Side chains were then added to the lowest-energy structures and energetically favorable conformations were obtained by varying side-chain torsional angles. Minimization was done with or without other CDRs being present. For all four CDRs, at least one of the low-energy models approximated the crystallographically determined structure with overall rms deviations in the backbones of about 1.0 Å.

Crystal structures are available for the Fabs of J539 (84), D1.3 (29), and HyHEL-10 (31), for which models of the combining sites had been constructed (132–134, 136) prior to the X-ray analysis. When the models are compared to the crystal structures, some of the CDR structures are found to have been, by and large, correctly predicted, while large disagreements between model and X-ray structure are found in other loops.

Comparison of the crystal structure of the J539 Fv (84) with the model of Mainhart et al (133) showed that the alpha carbon rms deviations for individual CDRs ranged from 1.1 Å to 4.0 Å (84). When the modeled hypervariable loops of D1.3 were compared with the crystal structure (29), the deviations of the model based on structural analysis ranged from 0.5 A to 2.07 A; the deviations of the models built using conformational energy calculations ranged from 0.47 A to 3.76 A (136). Comparing the model constructed for the Fv of HyHEL-10 (134) with the X-ray structure (31), deviations in C-alpha positions in the CDRs ranged from 0.44 A to 4.27 A (E. A. Padlan, unpublished results).

It is difficult to assess the success of these prediction algorithms. In most cases, crystal structures are not available to allow the comparison of model with X-ray structure. Even when crystal structures are available, their accuracies are frequently too low to permit a meaningful comparison with the models.

Most of the X-ray analyses of Fab structures have been done at medium resolution, i.e. between 2 Å and 3 Å. In these analyses, estimates of the error in atomic position in the most ordered regions, i.e., the most accurately determined parts of the molecule, are about half an angstrom; the error in the loop regions and for the side-chain atoms would be much larger. It is not unusual for a significant rebuilding of external regions to occur when a crystallographic analysis is extended to higher resolution. Indeed, when the analysis of the crystal structure of J539 Fab was extended to 1.95 Å resolution (T. N. Bhat, E. A. Padlan, and D. R. Davies, unpublished results), large

discrepancies were noted between the newly refined structure and that previously refined at 2.6 Å resolution (84); in this case, the three CDRs of the heavy chain had to be restructured, resulting in significant deviations between the old and the new structures, in one instance of more than 8 Å between two corresponding C-alpha positions. The large probable errors in low resolution crystal structures should serve to caution those who choose to define the hypervariable regions in terms of structural differences instead of sequence variation.

Future Directions

It is likely that modeling will eventually serve as a reliable predictor of combining site structures. However, for this to happen, more and better-refined X-ray structures will be needed. Fortunately, as reported above, there appears to be a considerable increase in the number of Fab structures being examined, and the application of molecular replacement methods (140) will facilitate the structure analyses. These new structures, some of which will be at higher resolution, will significantly enhance the data base available for modeling.

Already there are a number of structural invariants in antibodies that aid the modeller. Among these are the common tertiary fold of the domains (4–7, 48), the constancy of the domain interior volume (141, 142), the conservation of the VL-VH contact (13–17, 143) despite the involvement of CDRs in this interaction, and the similar structures of CDRs, especially those with the same number of residues (20, 126, 135, 144). All the structural results so far validate the notion that the different combining sites are constructed by draping different CDRs onto a highly conserved framework structure.

However, our knowledge of CDR loop structures is still quite inadequate. There are large variations in the lengths of some CDRs, specifically CDR1-L and CDR3-H (12), and only a few of these have been visualized by crystallography. Since it is unlikely that representative structures of all the various sorts of CDRs will be elucidated, it will be necessary to be able to predict three-dimensional structure on the basis of amino acid sequence. Presently, no procedure has been able to predict accurately the structure of a protein segment of any reasonable size.

Furthermore, the conformation of any given segment may exist in dynamic equilibrium among many different states. In fact, even in the same crystal, CDR loops with identical primary structures have been found to have different conformations (4). The influence of the environment is probably very important, so that, to model correctly the structure of a particular CDR in a combining site, it would be necessary to know how the conformation of that CDR is influenced by the neighboring structures. Some CDRs are long and

may be mostly exposed to solvent; predicting their structures would be extremely difficult.

It is encouraging that some of the models that have been built can account for many of the results of biochemical studies. In one case, a model of the combining site and of the complex of that site with ligand proved useful in predicting amino acid substitutions that resulted in enhanced affinity and specificity for the antigen (145). The evaluations of the structural changes that would result from the replacement of a small number of amino acids (e.g. 146, 147) are particularly useful in this regard.

ACKNOWLEDGMENTS

We thank Drs. Wayne Anderson, Louis Delbaere, Allen Edmundson, Robert Fox, Karl Hardman, James Herron, Alastair Muir, Roberto Poljak, Sandra Smith-Gill, William Tulip, Marc Whitlow, and Ian Wilson for providing preprints, coordinates, and other information prior to publication. We apologize to those authors whose work we have not cited; we have been limited by the size of the review to a discussion of results from X-ray analyses.

Literature Cited

1. Kindt, T. J., Capra, J. D. 1984. *The Antibody Enigma.* New York: Plenum
2. Edelman, G. M., Cunningham, B. A., Gall, W. E., Gottlieb, P. D., Rutishauser, U., Waxdal, M. J. 1969. *Proc. Natl. Acad. Sci. USA* 63:78–85
3. Edelman, G. M. 1970. *Biochemistry* 9:3197–205
4. Schiffer, M., Girling, R. L., Ely, K. R., Edmundson, A. B. 1973. *Biochemistry* 12:4620–31
5. Poljak, R. J., Amzel, L. M., Avey, H. P., Chen, B. L., Phizackerley, R. P., Saul, F. 1973. *Proc. Natl. Acad. Sci. USA* 70:3305–10
6. Epp, O., Colman, P., Fehlhammer, H., Bode, W., Schiffer, M., et al. 1974. *Eur. J. Biochem.* 45:513–24
7. Segal, D. M., Padlan, E. A., Cohen, G. H., Rudikoff, S., Potter, M., Davies, D. R. 1974. *Proc. Natl. Acad. Sci. USA* 71:4298–302
8. Williams, A. F., Barclay, A. N. 1988. *Annu. Rev. Immunol.* 6:381–405
9. Hunkapiller, T., Hood, L. 1989. *Adv. Immunol.* 44:1–63
10. Becker, J. W., Reeke, G. N. 1985. *Proc. Natl. Acad. Sci. USA* 82:4225–29
11. Bjorkman, P. J., Saper, M. A., Samraoui, B., Bennett, W. S., Strominger, J. L., Wiley, D. C. 1987. *Nature* 329:506–12
12. Kabat, E. A., Wu, T. T., Reid-Miller, M., Perry, H. M., Gottesman, K. S. 1987. *Sequences of Proteins of Immunological Interest.* Bethesda, Md: Natl. Inst. Health. 4th ed.
13. Poljak, R. J. 1975. *Adv. Immunol.* 21:1–33
14. Poljak, R. J. 1975. *Nature* 256:373–76
15. Poljak, R. J., Amzel, L. M., Chen, B. L., Phizackerley, R. P., Saul, F. 1975. *Philos. Trans. R. Soc. London, Ser. B* 272:43–51
16. Davies, D. R., Padlan, E. A., Segal, D. M. 1975. *Annu. Rev. Biochem.* 44:639–67
17. Davies, D. R., Padlan, E. A., Segal, D. M. 1975. In *Contemporary Topics in Molecular Immunology,* ed. F. P. Inman, W. J. Mandy, 4:127–55. New York: Plenum
18. Huber, R. 1976. *Trends. Biochem. Sci.* 1:174–78
19. Poljak, R. J., Amzel, L. M., Phizackerley, R. P. 1976. *Prog. Biophys. Mol. Biol.* 31:67–93
20. Padlan, E. A. 1977. *Q. Rev. Biophys.* 10:35–65
21. Amzel, L. M., Poljak, R. J. 1979. *Annu. Rev. Biochem.* 48:961–97
22. Davies, D. R., Metzger, H. 1983. *Annu. Rev. Immunol.* 1:87–117
23. Alzari, P. M., Lascombe, M.-B., Pol

jak, R. J. 1988. *Annu. Rev. Immunol.* 6:555–80
24. Amzel, L. M., Poljak, R. J., Saul, F., Varga, J. M., Richards, F. F. 1974. *Proc. Natl. Acad. Sci. USA* 71:1427–30
25. Padlan, E. A., Segal, D. M., Spande, T. F., Davies, D. R., Rudikoff, S., Potter, M. 1973. *Nature New Biol.* 145:165–67
26. Padlan, E. A., Davies, D. R., Rudikoff, S., Potter, M. 1976. *Immunochemistry* 13:945–49
27. Padlan, E. A., Cohen, G. H., Davies, D. R. 1985. *Ann. Inst. Pasteur/ Immunol.* 136C:259–94
28. Herron, J. N., He, X. M., Mason, M. L., Voss, E. W. Jr., Edmundson, A. B. 1989. *Proteins: Struct. Funct. Genet.* 5:271–80
29. Amit, A. G., Mariuzza, R. A., Phillips, S. E. V., Poljak, R. J. 1986. *Science* 233:747–53
30. Sheriff, S., Silverton, E. W., Padlan, E. A., Cohen, G. H., Smith Gill, S. J., et al. 1987. *Proc. Natl. Acad. Sci. USA* 84:8075–79
31. Padlan, E. A., Silverton, E. W., Sheriff, S., Cohen, G. H., Smith Gill, S. J., Davies, D. R. 1989. *Proc. Natl. Acad. Sci. USA* 86:5938–42
32. Colman, P. M., Laver, W. G., Varghese, J. N., Baker, A. T., Tulloch, P. A., et al. 1987. *Nature* 326:358–63
33. Tulip, W. R., Varghese, J. N., Webster, R. G., Air, G. M., Laver, W. G., Colman, P. M. 1989. *Cold Spring Harbor Symp. on Quant. Biol.* 54:257–63
34. Colman, P. M., Tulip, W. R., Varghese, J. N., Tulloch, P. A., Baker, A. T., et al. 1989. *Philos. Trans. R. Soc. London, Ser. B* 320:511–18
35. Jencks, W. P. 1969. *Catalysis In Chemistry And Enzymology*. New York: McGraw-Hill
36. Lerner, R. A., Tramontano, A. 1988. *Sci. Am.* 258(3):58–70
37. Schultz, P. G. 1988. *Science* 240:426–33
38. Koehler, G., Milstein, C. 1975. *Nature* 256:495–97
39. Boulianne, G. L., Hozumi, N., Schulman, M. J. 1984. *Nature* 312:643–46
40. Morrison, S. L., Johnson, M. J., Herzenberg, L. A., Oi, V. T. 1984. *Proc. Natl. Acad Sci. USA* 81:6851–55
41. Neuberger, M. S., Williams, G. T., Fox, R. O. 1984. *Nature* 312:604–8
42. Morrison, S. L., Oi, V. T. 1989. *Adv. Immunol.* 44:65–92
43. Jones, P. T., Dear, P. H., Foote, J., Neuberger, M. S., Winter, G. 1986. *Nature* 321:522–25
44. Verhoeyen, M., Milstein, C., Winter, G. 1988. *Science* 239:1534–36
45. Riechmann, L., Clark, M., Waldmann, H., Winter, G. 1988. *Nature* 332:323–27
46. Varga, J. M., Lande, S., Richards, F. F. 1974. *J. Immunol.* 112:1565–70
47. Potter, M. 1972. *Physiol. Rev.* 52:631–719
48. Poljak, R. J., Amzel, L. M., Chen, B. L., Phizackerley, R. P., Saul, F. 1974. *Proc. Natl. Acad. Sci. USA* 71:3440–44
49. Saul, F. A., Amzel, L. M., Poljak, R. J. 1978. *J. Biol. Chem.* 253:585–97
50. Satow, Y., Cohen, G. H., Padlan, E. A., Davies, D. R. 1986. *J. Mol. Biol.* 190:593–604
51. Potter, M., Lieberman, R. 1970. *J. Exp. Med.* 132:737–51
52. Leon, M. A., Young, N. M. 1971. *Biochemistry* 10:1424–29
53. Metzger, H., Chesebro, B., Hadler, N. M., Lee, J., Otchin, N. 1971. In *Progress in Immunology*, ed. B. Amos, pp. 253–67. New York: Academic
54. Lascombe, M. B., Alzari, P. M., Boulot, G., Saludjian, P., Tougard, P., et al. 1989. *Proc. Natl. Acad. Sci. USA* 86:607–11
55. Stura, E. A., Stanfield, R. L., Fieser, T. M., Balderas, R. S., Smith, L. R., et al. 1989. *J. Biol. Chem.* 264:15721–25
56. Sheriff, S., Smith, J. L., Hendrickson, W. A. 1987. *J. Mol. Biol.* 197:273–96
57. Schulze Gahmen, U., Rini, J. M., Arevalo, J., Stura, E. A., Kenten, J. H., Wilson, I. A. 1988. *J. Biol. Chem.* 263:17100–5
58. Stura, E. A., Feinstein, A., Wilson, I. A. 1987. *J. Mol. Biol.* 193:229–31
59. Stura, E. A., Arevalo, J. H., Feinstein, A., Heap, R. B., Taussig, M. J., Wilson, I. A. 1987. *Immunology* 62:511–21
60. Mariuzza, R. A., Phillips, S. E. V., Poljak, R. J. 1987. *Annu. Rev. Biophys. Biophys. Chem.* 16:139–59
61. Colman, P. M., Air, G. M., Webster, R. G., Varghese, J. N., Baker, A. T., et al. 1987. *Immunol. Today* 8:323–26
62. Davies, D. R., Sheriff, S., Padlan, E. A. 1988. *J. Biol. Chem.* 263:10541–44
63. Colman, P. M. 1988. *Adv. Immunol.* 43:99–132
64. Davies, D. R., Sheriff, S., Padlan, E. A. 1989. *Cold Spring Harbor Symp. Quant. Biol.* 54:233–38
65. Kundrot, C. E., Richards, F. M. 1987. *J. Mol. Biol.* 193:157–70
66. Imoto, T., Johnson, L. N., North, A. C.

T., Phillips, D. C., Rupley, J. A. 1972. *The Enzymes* 7:665
67. Blake, C. C F., Koenig, D. F., Mair, G. A., North, A. C. T., Phillips, D. C., Sarma, V. R. 1965. *Nature* 206:757–61
68. Ramanadhan, M., Sieker, L. C., Jen sen, L. H. 1989. See Ref. 75, p. 15
69. Yu, C., Rao, S. T., Sundaralingam, M. 1989. See Ref. 75, p. 25
70. Artymiuk, P. J., Blake, C. C. F. 1981. *J. Mol. Biol.* 152:737 62
71. Blake, C. C. F., Pulford, W. C. A., Artymiuk, P. J. 1983. *J. Mol. Biol.* 167:693 723
72. Arnon, R. 1977. In *Immunochemistry of Enzymes and Their Antibodies*, ed. M. R. J. Salton, pp. 1 28. New York: Wiley
73. Atassi, M. Z. 1978. *Immunochemistry* 12:423 38
74. Benjamin, D. C., Berzofsky, J. A., East, I. J., Gurd, F. R. N., Hannum, C., et al. 1984. *Annu. Rev. Immunol.* 2:67 101
75. Smith Gill, S. J., Sercarz, E. E., eds. 1989. *The Immune Response to Structurally Defined Proteins. The Lysozyme Model.* New York: Adenine
76. Bentley, G. A., Bhat, T. N., Boulot, G., Fischmann, T., Navaza, J., et al. 1989. *Cold Spring Harbor Symp. Quant. Biol.* 54:239 45
77. Smith-Gill, S. J., Wilson, A. C., Potter, M., Prager, E. M., Feldmann, R. J., Mainhart, C. R. 1982. *J. Immunol.* 128:314 22
78. van Regenmortel, M. H. V. 1989. *Philos. Trans. R. Soc. London, Ser. B* 323:451 66
79. Getzoff, E. D., Geysen, H. M., Rodda, S. J., Alexander, H., Tainer, J. A., Lerner, R. A. 1987. *Science* 235:1191 96
80. Getzoff, E. D., Tainer, J. A., Lerner, R. A., Geysen, H. M. 1988. *Adv. Immunol.* 43:1 98
81. Miller, S., Lesk, A. M., Janin, J., Chothia, C. 1987. *Nature* 328:834 36
82. Kauzmann, W. 1959. *Adv. Protein Chem.* 14:1 63
83. Varghese, J. N., Laver, W. G., Col man, P. M. 1983. *Nature* 303:35 40
84. Suh, S. W., Bhat, T. N., Navia, M. N., Cohen, G. H., Rao, D. N., et al. 1986. *Proteins: Struct. Funct. Genet.* 1:74 80
85. Vitali, J., Young, W. W., Schatz, V. B., Sobottka, S. E., Kretsinger, R. H. 1987. *J. Mol. Biol.* 198:351 55
86. Cygler, M., Boodhoo, A., Lee, J. S., Anderson, W. F. 1987. *J. Biol. Chem.* 262:643 48
87. Gibson, A. L., Herron, J. N., Ballard, D. W., Voss, E. W. Jr., He, X. M., et al. 1985. *Mol. Immunol.* 22:499–502
88. Boodhoo, A., Mol, C. D., Lee, J. S., Anderson, W. F. 1988. *J. Biol. Chem.* 263:18578 81
89. Prasad, L., Vandonselaar, M., Lee, J. S., Delbaere, L. T. J. 1988. *J. Biol. Chem.* 263:2571 74
90. Delbaere, L. T. J., Vandonselaar, M., Quail, J. W., Waygood, E. B., Lee, J. S. Submitted
91. Novotny, J., Bruccoleri, R. E., Saul, F. A. 1989. *Biochemistry* 28:4735–49
92. Padlan, E. A. 1989. *Proteins: Struct. Funct. Genet.* In press
93. Chaudhary, V. K., Queen, C., Jung hans, R. P., Waldmann, T. A., Fitzgerald, D. J., Pastan, I. 1989. *Nature* 339:394 97
94. Bird, R. E., Hardman, K. D., Jacobson, J. W., Johnson, S., Kaufman, B. M., et al. 1988. *Science* 242:423 26
95. Huston, J. S., Levinson, D., Mudgett Hunter, M., Tai, M.-S., Novotny, J., et al. 1988. *Proc. Natl. Acad. Sci. USA* 85:5879 83
96. Liu, A. Y., Robinson, R. R., Hellstrom, K. E., Murray, E. D. Jr., Chang, C. P., Hellstrom, I. 1987. *Proc. Natl. Acad. Sci. USA* 84:3439–43
97. Ehrlich, P. 1900. *Proc. R. Soc. London Ser. B.* 66:424 48
98. Pauling, L. 1948. *Am. Sci.* 36:51–58
99. Burd, J. F., Carrico, R. J., Fetter, M. C., Buckler, R. T., Johnson, R. D. 1977. *Anal. Biochem.* 77:56–67
100. Kohen, F., Kim, J. B., Lindner, H. R., Eshhar, Z., Green, B. 1980. *FEBS Lett.* 111:427 31
101. Kohen, F., Hollander, Z., Burd, J. F., Boguslaski, R. C. 1979. *FEBS Lett.* 100:137 40
102. Kohen, F., Kim, J. B., Barnard, G., Lindner, H. R. 1980. *Biochim. Biophys. Acta* 629:328 37
103. Tramontano, A., Janda, K. D., Lerner, R. A. 1986. *Science* 234:1566–70
104. Pollack, S. J., Jacobs, J. W., Schultz, P. G. 1986. *Science* 234:1570 73
105. Tramontano, A., Ammann, A. A., Lerner, R. A. 1988. *J. Am. Chem. Soc.* 110:2282 86
106. Janda, K. D., Benkovic, S. J., Lerner, R. A. 1989. *Science* 244:437 40
107. Jacobs, J., Schultz, P. G. 1987. *J. Am. Chem. Soc.* 109:2174 76
108. Napper, A. D., Benkovic, S. J., Tra montano, A., Lerner, R. A. 1987. *Science* 237:1041 43
109. Jackson, D. Y., Jacobs, J. W., Sugasa wara, R., Reich, S. H., Bartlett, P. A.,

Schultz, P. G. 1988. *J. Am. Chem. Soc.* 110:4841 42
110. Hilvert, D., Nared, K. D. 1988. *J. Am. Chem. Soc.* 110:5593 94
111. Hilvert, D., Carpenter, S. H., Nared, K. D., Auditor, M. T. M. 1988. *Proc. Natl. Acad. Sci. USA* 85:4953 55
112. Janda, K. D. Lerner, R. A., Tramontano, A. 1988. *J. Am. Chem. Soc.* 110:4835 37
113. Benkovic, S. J., Napper, A. D., Lerner, R. A. 1988. *Proc. Natl. Acad. Sci. USA* 85:5355 58
114 Janda, K. D., Schloeder, D., Benkovic, S. J. Lerner, R. A. 1988. *Science* 241:1188 91
115. Cochran, A. G., Sugasawara, R., Schultz, P. G. 1988. *J. Am. Chem. Soc.* 110:7888–90
116. Shokat, K. M., Leumann, C. J., Sugasawara, R., Schultz, P. G. 1988. *Angew. Chem. Int. Ed. Engl.* 27:1172 74
117. Iverson, B. L., Lerner, R. A. 1989. *Science* 243:1184 88
118. Shokat, K. M., Leumann, C. J. Sugasawara, R., Schultz, P. G. 1989. *Nature* 338:269–71
119. Paul, S., Volle, D. J., Beach, C. M., Johnson, D. R., Powell, M. J., Massey, R. J. 1989. *Science* 244:1158 62
120. Pollack, S. J., Nakayama, G. R., Schultz, P. G. 1988. *Science* 242:1038 40
121. Lerner, R. A., Tramontano, A. 1987. *Trends Biochem. Sci.* 12:427–30
122. Massey, R. J. 1987. *Nature* 328:457 58
123. Kabat, E. A., Wu, T. T. 1972. *Proc. Natl. Acad. Sci. USA* 69:960 64
124. Padlan, E. A., Davies, D. R., Pecht, I., Givol, D., Wright, C. 1976. *Cold Spring Harbor Symp. Quant. Biol.* 41:627 37
125. Fehlhammer, H., Schiffer, M., Epp, O., Colman, P. M., Lattman, E. E., et al. 1975. *Biophys. Struct. Mech.* 1:139 46
126. Padlan, E. A., Davies, D. R. 1975. *Proc. Natl. Acad. Sci. USA* 72:819 23
127. Dower, S., Wain Hobson, S., Gettins, P., Givol, D., Jackson, W. R. C., et al. 1977. *Biochem. J.* 165:207 25
128. Dwek, R. A., Wain Hobson, S., Dower, S., Gettins, P., Sutton, B., Perkins, S. J. 1977. *Nature* 266:31 37
129. Davies, D. R., Padlan, E. A. 1977. In *Antibodies In Human Diagnosis And Therapy*, ed. E. Haber, R. M. Krause, pp. 119–132. New York: Raven
130. Potter, M., Rudikoff, S., Padlan, E. A., Vrana, M. 1977. See Ref. 129, pp. 9 28
131. Padlan, E. A., Kabat, E. A. 1988. *Proc. Natl. Acad. Sci. USA* 85:6885 89
132. Feldmann, R. J., Potter, M., Glaudemans, C. P. J. 1981. *Mol. Immunol.* 18:683 98
133. Mainhart, C. R., Potter, M., Feldmann, R. J. 1984. *Mol. Immunol.* 21:469 78
134. Smith-Gill, S. J., Mainhart, C., Lavoie, T. B., Feldmann, R. J., Drohan, W., Brooks, B. R. 1987. *J. Mol. Biol.* 194:713 24
135. de la Paz, P., Sutton, B. J., Darsley, M. J., Rees, A. R. 1986. *EMBO J.* 5:415 25
136. Chothia, C., Lesk, A. M., Levitt, M., Amit, A. G., Mariuzza, R. A., et al. 1986. *Science* 233:755 58
137. Stanford, J. M., Wu, T. T. 1981. *J. Theor. Biol.* 88:421 39
138. Bruccoleri, R. E., Haber, E., Novotny, J. 1988. *Nature* 335:564 68
139. Fine, R. M., Wang, H., Shenkin, P. S., Yarmush, D. L., Levinthal, C. 1986. *Proteins Struct. Funct. Genet.* 1:342 62
140. Rossmann, M. G., ed. 1972. *The Molecular Replacement Method.* New York: Gordon & Breach
141. Padlan, E. A. 1979. *Mol. Immunol.* 16:287 96
142. Novotny, J., Haber, E. 1985. *Proc. Natl. Acad. Sci. USA* 82:4592 96
143. Chothia, C., Novotny, J., Bruccoleri, R., Karplus, M. 1985. *J. Mol. Biol.* 186:651 63
144. Chothia, C., Lesk, A. M. 1987. *J. Mol. Biol.* 196:901 17
145. Roberts, S., Cheetham, J. C., Rees, A. R. 1987. *Nature* 328:731 34
146. Snow, M. E., Amzel, L. M. 1986. *Proteins Struct. Funct. Genet.* 1:267 79
147. Chien, N. V., Roberts, V. A., Giusti, A. M., Scharff, M. D., Getzoff, E. D. 1989. *Proc. Natl. Acad. Sci. USA* 86:5532 36
148. Case, D. A., Karplus, M. 1979. *J. Mol. Biol.* 132:343 68
149. Connolly, M. L. 1983. *J. Appl. Crystallogr.* 16:548 58
150. Deleted in proof
151. Janin, J., Miller, S., Chothia, C. 1988. *J. Mol. Biol.* 204:155 64
152. Deisenhofer, J. 1981. *Biochemistry* 20: 2361 70
153. Marquart, M., Deisenhofer, J., Huber, R., Palm, W. 1980. *J. Mol. Biol.* 141:369 91
154. Holmgren, A., Branden, C. I. 1989. *Nature* 342:248 51

Annual Review of Biochemistry
Volume 59, 1990

CONTENTS